How to Make Water Run Uphill

Manoj K. Chaudhury; George M. Whitesides

Science, New Series, Vol. 256, No. 5063 (Jun. 12, 1992), 1539-1541.

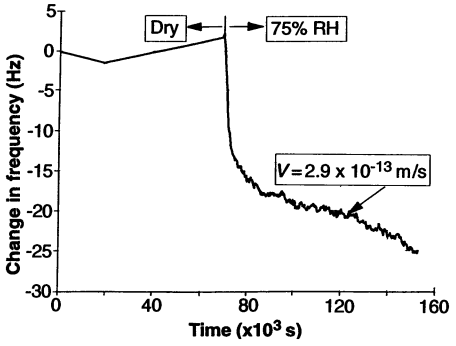

Fig. 4. Change in resonant frequency upon the addition of humid air; RH, relative humidity. The change in frequency represents immediate crack growth.

The actual mechanism governing the rate-dependent crack growth in silicon has not been well characterized. The crack growth rate does not accelerate with increasing crack length, which indicates that this rate is independent of the magnitude of the stress intensity. One possible explanation for this independence is some rate-limiting mechanism associated with either reaction rates at the crack tip or delivery of species from or to the crack tip region.

Several difficulties with the current device remain to be resolved. First, although we have good correlation between the model and device behavior, we believe that it is important to model the structure in its actual nonlinear form. Second, the stress intensity estimates assume a deep cracked beam with rectangular cross section. The actual cross section of the beam deviates from a true rectangle. Third, because we deduce crack growth from frequency shifts, we need to perform measurements of crack length based on interrupted experiments in which we measure crack length by breaking and examining fracture surfaces, using a method to mark the exposed crack, or by static compliance using a nanoindenter as a force-displacement test machine.

We have concentrated on doped, single-crystal silicon in this initial effort because in this way we eliminated the complexity associated with deposited microstructures had we used polysilicon or some other polycrystalline material. The susceptibility to rate-dependent failure should increase with polycrystalline microstructures (*17*). Moreover, dynamic fatigue will definitely be possible in materials that have greater dislocation mobilities than silicon.

REFERENCES AND NOTES

1. K. D. Wise and K. Najafi, *Science* **254**, 1335 (1991).
2. T. A. Michalske and B. C. Bunker, *J. Appl. Phys.* **56**, 2686 (1984).
3. S. M. Wiederhorn, *Fracture Mech. Ceram.* 1974, 613 (1974).
4. T.-J. Chen and W. J. Knapp, *J. Am. Ceram. Soc.* **63**, 225 (March 1980).
5. B. Wong and R. J. Holbrook, *J. Electrochem. Soc.* **134**, 2254 (1987).
6. S. B. Bhaduri and F. F. Y. Wang, *Fracture Mech. Ceram.* **1983**, 327 (1983).
7. C. P. Chen and M. H. Leipold, *NASA Tech. Brief* **10**, Item 106 (1986).
8. M. D. Thouless and R. F. Cook, *Appl. Phys. Lett.* **56**, 1962 (1990).
9. T. P. Weihs, S. Hong, J. C. Bravman, W. D. Nix, *J. Mater. Res.* **3**, 931 (1988).
10. S. Johansson, J. Schweitz, L. Tenerz, J. Tiren, *J. Appl. Phys.* **63**, 4799 (1988).
11. L. Fan, R. T. Howe, R. S. Muller, in *IEEE Micro-Electro-Mechanical Systems Workshop*, 20 to 22 February 1989, Salt Lake City (IEEE, Piscataway, NJ, 1989), p. 40.
12. S. Murakami, *Stress Intensity Factors Handbook* (Pergamon, Elmsford, NY, 1987).
13. J. A. Connally and S. B. Brown, in *Proceedings of the Sixth International Conference on Sensors and Actuators* (IEEE, Piscataway, NJ, 1991), p. 953.
14. D. Broek, *Elementary Engineering Fracture Mechanics* (Sijthoff & Hoordhoff, Alphen aan den Rijn, The Netherlands, 1978), chap. 13.
15. C. P. Chen and M. H. Leipold, *Am. Ceram. Soc. Bull.* **59**, 469 (1980).
16. S. K. Ghandhi, *VLSI Fabrication Principles* (Wiley, New York, 1983), chap. 7.
17. L. Ewart and S. Suresh, *J. Mater. Sci.* **22**, 1173 (1987).

18. We acknowledge the support of the Charles Stark Draper Laboratories and the particular assistance of B. Boxenhorn and P. Greiff. Substantial assistance was also provided by A. Taylor of AT&T Laboratories and M. Ferber of the High Temperature Materials Laboratory at Oak Ridge National Laboratory.

28 February 1992; accepted 17 April 1992

How to Make Water Run Uphill

Manoj K. Chaudhury and George M. Whitesides

A surface having a spatial gradient in its surface free energy was capable of causing drops of water placed on it to move uphill. This motion was the result of an imbalance in the forces due to surface tension acting on the liquid-solid contact line on the two opposite sides ("uphill" or "downhill") of the drop. The required gradient in surface free energy was generated on the surface of a polished silicon wafer by exposing it to the diffusing front of a vapor of decyltrichlorosilane, $Cl_3Si(CH_2)_9CH_3$. The resulting surface displayed a gradient of hydrophobicity (with the contact angle of water changing from 97° to 25°) over a distance of 1 centimeter. When the wafer was tilted from the horizontal plane by 15°, with the hydrophobic end lower than the hydrophilic, and a drop of water (1 to 2 microliters) was placed at the hydrophobic end, the drop moved toward the hydrophilic end with an average velocity of ~1 to 2 millimeters per second. In order for the drop to move, the hysteresis in contact angle on the surface had to be low (≤10°).

The motion of liquid drops on surfaces that is induced by thermal gradients has been observed experimentally and discussed theoretically (*1–4*). This type of drop motion is a consequence of the Marangoni flow within the drop that is set up by thermal gradients. Motion of liquid driven by Marangoni flow is also evident in the classical "tear of wine" effect (*5*). Evaporation of alcohol from the liquid-solid meniscus creates a local rise of the surface tension in the liquid, which induces a surface flow (and in turn a bulk flow) of wine on the wall of the wine glass; the accumulating liquids return in the form of drops. Cottington *et al.* reported that drops of several oils moved freely on a stainless steel surface when the oils contained certain types of surfactant additives (*6*). The authors postulated that the nonuniform evaporation of the surfactant resulted in a surface tension gradient in the liquid drop; this gradient caused the drops to move. This motion appears to be another example of the Marangoni effect.

M. K. Chaudhury, Dow Corning Corporation, Midland, MI 48686.
G. M. Whitesides, Department of Chemistry, Harvard University, Cambridge, MA 02138.

We report a new type of drop motion that is induced entirely by a surface chemical gradient of a solid substrate. What distinguishes the motion described here from the motions reported earlier (*1, 2, 4–6*) is the fact that no Marangoni forces act on the liquid—instead, the motion results from the imbalance of the surface tension forces acting on the opposite sides of the drop edge. Figure 1 represents a cross section of a water drop placed on a surface that has a spatial gradient in the surface free energy. The unbalanced Young's force (dF_Y) experienced by this section of the drop is given by Eq. 1

$$dF_Y = [(\gamma_{SV} - \gamma_{SL})_A - (\gamma_{SV} - \gamma_{SL})_B]dx \quad (1)$$

Here, γ_{SV} and γ_{SL} are the surface free energies of the solid-vapor and solid-liquid interfaces and dx is the thickness of the section of the drop. If θ_A and θ_B represent the local contact angles at points A and B, then Eq. 1 can be represented as

$$dF_Y = \gamma_{LV}(\cos\theta_A - \cos\theta_B)dx \quad (2)$$

The surface free energy of the liquid-vapor interface is γ_{LV}. The net force (F_Y) experi-

enced by the drop can be obtained by integrating Eq. 2 over the entire width of the drop. If the contact angle at point A is smaller than that at point B, the drop will move in the direction of higher γ_{SV}. This motion has two effects: it decreases the area of the vapor-solid interface having the larger interfacial free energy while increasing that having lower free energy, and it increases the total area of solid-liquid interface. Both changes in free energy, effected over a distance, constitute a force driving the drop uphill against the force of gravity. For a surface that exhibits high hysteresis in contact angles, however, the receding contact angle at point B may become smaller than the advancing contact angle at point A. Under this condition the drop will not move (*3*, *7*). The presence of a gradient in surface tension is thus not, by itself, sufficient to ensure motion of liquid drops—the surface must also have low hysteresis in contact angles and be free of defects that pin the edge of the drop (*8*).

The method we used to produce gradients in chemical compositions and surface tension on solid surfaces is a modification of the method developed by Elwing *et al.* (*9*). It is based on allowing the surface of a silicon wafer to react with vapors of a volatile alkylchlorosilane by using a diffusion-controlled process. The silanization reactions reported by Elwing *et al.* were carried out in solvents, and the resulting wafers exhibited large hystereses in contact angles (20° to 40°) (*10*). We used a method that generates gradient surfaces of lower hysteresis (6° to 8°). This combination of gradient and hysteresis caused 1- to 2-μl drops of water to move up a 15° slope along the direction of increasing surface free energy, with average velocities of 1 to 2 mm/s (*11*).

The gradient surface was prepared by allowing the vapor of decyltrichlorosilane [$Cl_3Si(CH_2)_9CH_3$, or $RSiCl_3$] to diffuse over a silicon wafer (Fig. 2). A clean (*12*) silicon wafer was placed 2 mm from a solution of $RSiCl_3$ in paraffin oil. As the silane evaporated and diffused in the vapor phase, it generated a gradient of concentration that decreased along the length of the wafer. The profile of this gradient was imprinted onto the silicon wafer by reaction with its surface. The edge of the wafer closest to the silane became hydrophobic; the farthest edge remained hydrophilic. The steepness of the gradient was a function of the time of exposure of the wafer to the vapor of the silane. After the formation of the chemical gradient, the wafer was placed in warm distilled water (65°C) for 1 min, rinsed thoroughly in running distilled water, and stored in distilled water at room temperature (*13*).

The gradient surfaces were characterized with contact-angle measurements and ellipsometry. The typical wettability gradient produced by exposing the wafer to vapors of $RSiCl_3$ for 5 min is shown in Fig. 2. The contact angles decreased smoothly (*14*); the hysteresis of contact angles was ~10° on the hydrophobic edge of the wafer and 6° to 8° for most of the gradient but increased abruptly at the hydrophilic end. The thickness of the alkylsiloxane layer, obtained by ellipsometry, was ~6 Å (*15*) at the hydrophobic end of the gradient. This value indicates that the layer is significantly less than a monolayer and is disordered (*16*). The thickness decreased steadily at a rate of ~1 Å/mm up to a distance of 5 mm from the hydrophobic edge, beyond which the estimation of thickness by ellipsometry became unreliable. Measurements of contact angles indicated that a gradient was present up to a distance of 1 cm from the hydrophobic edge.

The motion of water drops was examined by placing them on the hydrophobic edge of the gradient surface. The uphill motion of a water drop on a gradient surface

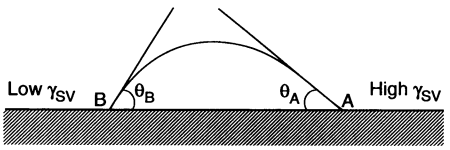

Fig. 1. Idealized diagram of a thin cross section of a liquid drop on a gradient surface. Although this diagram is useful for understanding the origin of Young's driving force on a gradient surface, it does not state the problem completely. Such a distorted drop shape would imply the presence of a Laplace pressure gradient within the drop. The pressure inside the drop would equalize, and the drop would assume the shape of a spherical cap. The value of the dynamic contact angle would be between θ_A and θ_B.

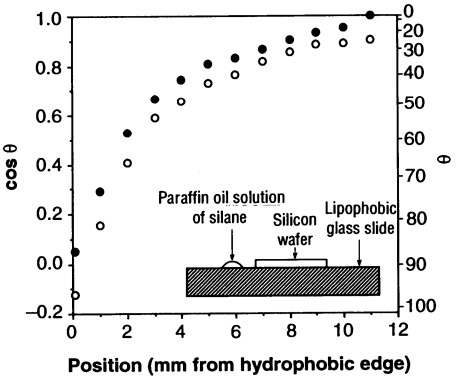

Fig. 2. Gradient in water wettability produced on a silicon wafer by 5-min exposure to diffusing vapor of $RSiCl_3$. The circles represent the advancing (○) and receding (●) contact angles of water. In the inset, the method used to form gradients in surface tension is illustrated schematically. The glass slide was initially silanized with $Cl_3Si(CH_2)_2(CF_2)_7CF_3$, which rendered it lipophobic. A small strip (3 mm wide) of this slide was oxidized in plasma; this strip was used to contain the solution of $RSiCl_3$. The solution of $RSiCl_3$ (30 μl of the silane solution, which contained 75 μl of silane per gram of paraffin oil) was placed within this strip. A clean silicon wafer (12 mm by 40 mm) was placed 2 mm from the edge of the silane solution. The gradient surface resulted from the diffusion of the silane in the vapor phase and subsequent reaction with the surface SiOH groups and adsorbed water on the silicon wafer. The whole assembly was placed in a polystyrene petri dish and covered. The relative humidity of the room was 40% during these experiments.

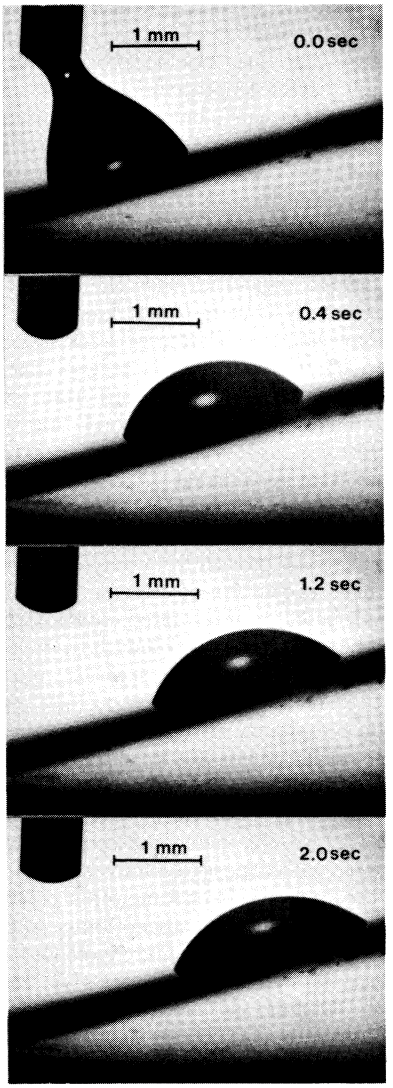

Fig. 3. Uphill motion of a drop of water on a gradient surface. The gradient surface was inclined by ~15° from the horizontal plane. The volume of the drop was ~1 μl. The moving drop was photographed with an automatic camera that exposed one frame every 0.4 s. The drop moved more rapidly on the initial part of the gradient than on the final part.

that was inclined by 15° from the horizontal plane is shown in Fig. 3. The speeds of the drops varied across the gradient and with the size of the drop; average speeds of 1 to 2 mm/s were observed for 1- to 2-μl drops on the steeper part of the gradient (*17*). The shape of the drop shown in Fig. 3 is that of a spherical cap. The difference of the contact angles in the advancing and receding edges of the drop was only ~2° to 3°. The effect of gravity on the drop shape was not significant here because the radius of the drop (1 to 1.5 mm) was smaller than the Laplace length (2.7 mm) (*18*). The near-spherical shape of the drop appears to be a consequence of the equilibration of the Laplace pressure inside the drop, which is consistent with the model proposed by Brochard (*3*).

Water was not the only liquid that moved across such gradient surfaces; other liquids such as glycerol and chloroform also moved. The motion of these liquids was, however, examined with a horizontal gradient surface.

Although we have not studied these factors in any detail, the speeds of the liquid drops depended on the hysteresis in contact angles, the surface tension and viscosity of the drops, the drop volume, the steepness of the gradient, and the inclination of the gradient surface. Detailed understanding of the kinetics of drop motion on gradient surfaces should take these factors into account. The gradient surfaces reported here are easily prepared. They should be useful in the study of the motion of liquid drops induced by chemical gradients and of the interplay of chemical and thermal gradients.

REFERENCES AND NOTES

1. H. Bouasse, *Capillarité et Phénomènes Superficielles* (Delagrave, Paris, 1924).
2. N. O. Young, J. S. Goldstein, M. J. Block, *J. Fluid Mech.* **6**, 350 (1959).
3. F. Brochard, *Langmuir* **5**, 432 (1989).
4. K. D. Barton and R. S. Subramanian, *J. Colloid Interface Sci.* **133**, 211 (1989).
5. A. W. Adamson, *Physical Chemistry of Surfaces* (Wiley, New York, ed. 3, 1976).
6. R. L. Cottington, C. M. Murphy, C. R. Singleterry, *Adv. Chem. Ser.* **43**, 341 (1964).
7. E. Raphael, *C. R. Acad. Sci. Paris Ser. II* **306**, 751 (1988).
8. T. Ondarcuhu and M. Veyssie, *J. Phys. (Paris) II* **1**, 75 (1991).
9. H. Elwing, S. Welin, A. Askendal, U. Nilsson, I. Lundstrom, *J. Colloid Interface Sci.* **119**, 203 (1987).
10. C.-G. Golander, Y.-S. Lin, V. Hlady, J. D. Andrade, *Colloids Surf.* **49**, 289 (1990).

11. These values of speed are approximate and variable. The effects of drop volumes on speeds have not been rigorously examined. Qualitatively, it was observed that the speeds increased as the volume of the drops increased.
12. Silicon wafers were cleaned in hot piranha solution, which is a mixture of 70% H_2SO_4 and 30% H_2O_2 (30% solution in water). The wafer was placed in this solution for 30 min. Afterward, the wafer was thoroughly rinsed with and stored in distilled water. Before we prepared the gradient surface, the wafer was rinsed again in running distilled water and then dried by blowing nitrogen over it.
13. We found that immersing the wafer in warm distilled water and rinsing it in pure distilled water helped to remove some of the loosely adsorbed contamination from the surface. The gradient surface can be easily contaminated by atmospheric impurities. The surface remained clean, however, when kept immersed in pure distilled water.
14. Drops used to measure the advancing and receding contact angles were held stationary on the surface of the silicon wafer by the tip of the microsyringe used to form the drops. The contact angles were measured under quasistatic conditions, that is, after the cessation of the movement of the contact line. For quantitative correlation between drop velocity and surface energy gradient, the contact angles should be measured under dynamic conditions. These measurements are beyond the scope of this study.
15. The thickness gradients of the monolayers were functions of the adsorption times and molecular weights of the silanes. We have also prepared gradient surfaces with $Cl_3Si(CH_2)_7CH_3$. After a 5-min adsorption, a close-packed, nearly complete monolayer (11 Å thick) was formed at the hydrophobic edge.
16. The thickness obtained by ellipsometry was an average over an area of ~3 mm^2.
17. The length (5 mm) of this gradient corresponds to what was detected by ellipsometry, which also matched the field of view of the telescope used to observe the motion of water drops. When the drop moved beyond 5 mm from the hydrophobic edge, the drop became flat and thin in the region of weaker gradient.
18. The Laplace length (also known as the capillary length) is $(\gamma_{LV}/\rho g)^{0.5}$, where ρ is the density of the liquid and g is the acceleration due to gravity.

19. M.K.C. acknowledges support from Dow Corning Corporation. G.M.W. acknowledges support from the Office of Naval Research and the Defense Advanced Research Projects Agency. We thank M. J. Owen (Dow Corning) for many valuable discussions.

9 January 1992; accepted 15 April 1992

Observation of Transition-State Vibrational Thresholds in the Rate of Dissociation of Ketene

Edward R. Lovejoy, Sang Kyu Kim, C. Bradley Moore

Rate constants for the dissociation of highly vibrationally excited ketene (CH_2CO) have been measured at the threshold for the production of $CH_2(^3B_1)$ and $CO(^1\Sigma^+)$. The rate constant increases in a stepwise manner with increasing energy, consistent with the long-standing premise that the rate of a unimolecular reaction is controlled by flux through quantized transition-state thresholds. The data give the energies of the torsional and C–C–O bending vibrations of the transition state.

The elementary chemical reaction is one of the most fundamental processes in nature, and the theoretical and experimental study of the transformation of reactants into products has been an important area of research for many decades. Experimental studies of unimolecular reactions of highly energized molecules provide strong tests of the theories developed to describe chemical reactivity (*1*). The unimolecular rate theory of Rice, Ramsperger, Kassel, and Marcus (RRKM) (*2*) is based on the assumptions that (i) the vibrational energy in the excited molecule is distributed statistically among all the vibrational degrees of freedom, (ii) the energy flows freely among the different degrees of freedom at a rate much faster than the reaction rate, and (iii) the rate of reaction is controlled by the passage through a transition state located at the dynamical bottleneck separating the reactant from products on the potential energy surface for the reaction. In the region of the transition state, the bound vibrational motions of the molecule are not coupled to the reaction coordinate, and passage through the transition state is vibrationally adiabatic. In this sense, the vibrational levels of the transition state represent reaction thresholds, that is, quantized channels connecting the reactant to products.

Chemical Sciences Division of the Lawrence Berkeley Laboratory and Department of Chemistry, University of California, Berkeley, CA 94720.

The energy dependence of the RRKM rate constant for a molecule with a fixed energy (E) and total angular momentum (J) is given by

$$k(E,J) = W^{\ddagger}(E,J)/[h\rho(E,J)] \quad (3)$$

where $W^{\ddagger}(E,J)$ is the number of vibrational levels of the transition state with energy less than E, $\rho(E,J)$ is the density of vibrational states of the reactant (number of states per unit energy), and h is Planck's constant.

Definitive tests of RRKM theory are hampered by the difficulty in evaluating the individual terms in Eq. 1. Historically, the density of reactant states [$\rho(E,J)$] has been estimated by extrapolating a normal mode treatment of the molecular vibrations to higher energies (*3*). However, recent spectroscopic studies show that the actual density of states for a number of molecules is significantly higher (five to ten times for $10{,}000\ cm^{-1} < E < 30{,}000\ cm^{-1}$) (*4*) than predicted by the normal mode picture. The number of accessible reaction channels at